



Dynamics of the Mediterranean droughts from 850 to 2099 AD in the Community Earth System Model

Woon Mi Kim^{1,2} and Christoph C. Raible^{1,2}

¹Climate and Environmental Physics, University of Bern, Switzerland

²Oeschger Centre for Climate Change Research, University of Bern, Switzerland

Correspondence: Woon Mi Kim (woonmi.kim@climate.unibe.ch)

Abstract.

In this study, we analyze the dynamics of multi-year long droughts over the western and central Mediterranean region for the period of 850 - 2099 AD using the Community Earth System model version 1.0.1. Our study indicates that Mediterranean droughts during the period of 850 - 1849 AD are mainly driven by the internal variability of the climate system. A barotropic high pressure system together with a positive temperature anomaly over central Europe and the Mediterranean is the prominent pattern that occurs in all seasons with droughts. Modes of variability, i.e. the North Atlantic Oscillation and El Niño Southern-Oscillation, play an important role at the initial stage of droughts. However, the persistence of multi-year droughts is determined by the interaction between the regional atmospheric and soil moisture variables. This interaction becomes stronger during the 1850 - 2099 AD period, reducing the importance of modes of variability and inducing a constant dryness over the Mediterranean region. Additionally, the discrepancy among diverse drought metrics in representing past droughts is shown, re-affirming the necessity of assessing a variety of drought indices even in the paleoclimate context.

1 Introduction

Drought is an extreme weather and climate event characterized by a prolonged period with persistent depletion of atmospheric moisture and surface water balance from its mean average condition. Drought is also characterized by a slow onset and devastating impacts on society, the economy and the environment (Wilhite, 1993; Dai, 2011, 2013). The severity and duration of a drought can be quantified through different indices that capture hydrological conditions associated with a regional water balance (Mishra and Singh, 2010; Dai, 2011). However, a single universal index cannot characterize the entire complexity of the nature of droughts (Lloyd-Hughes, 2014). Thus, one index does not necessarily produce a value that is similar to other indices even for the same region and period (Raible et al., 2017; Mukherjee et al., 2018). Some of the widely used indices are the self-calibrated Palmer Drought Severity Index (Wells et al., 2004), the Standardized Precipitation Index (McKee et al., 1993), and the Standardized Precipitation Evapotranspiration Index (Vicente-Serrano et al., 2009), among many others.

The Mediterranean region is known as a climate hot-spot. It is one of the most responsive regions to current and future global warming, mainly associated with the decrease in precipitation and increase in drought episodes, which would lead to a shortage of water availability in the region (Giorgi, 2006; Liu et al., 2018). The climate of the region is characterized as a



25 typical Mediterranean climate with mild and wet winters, and hot and dry summers, and the regional precipitation is strongly
influenced by modes of variability, such as the North Atlantic Oscillation (NAO), East Atlantic - West Russian pattern (EA
- WR) and El Niño-Southern Oscillation (ENSO) (Lionello et al., 2006). The NAO exerts its control on precipitation by in-
fluencing the strength of westerlies and latitudinal movement of the storm tracks. This influence largely becomes stronger
during the wintertime. The precipitation decreases during the positive NAO, mostly in the western Mediterranean region, and
30 the opposite condition occurs during the negative NAO (Wallace and Gutzler, 1981; Hurrell, 1995; Trigo et al., 2002). The
influence of EA-WR in European hydroclimate is also stronger in the winter. During the positive (negative) phase, the south-
eastern Mediterranean region experiences drier (wetter) condition than on average. The mechanism associated with the change
in precipitation is the advection of air masses from central Europe (the Atlantic) to the southeastern Mediterranean during
the positive (negative) phase (Barnston and Livezey, 1987; Krichak and Alpert, 2005). Additionally, the EA-WR presents a
35 non-linear interaction with the eastward shifted center of positive NAO, and it explains the precipitation signals over the region
which cannot be attributed to the NAO (Ulbrich and Christoph, 1999; Krichak and Alpert, 2005; Lionello et al., 2006). The
response of the Mediterranean climate on ENSO is more complex and not straightforward: it varies over time, discussed for
a few historical cases, and it depends on the maturity of the ENSO state, the season and the co-occurrence with phases of
the NAO (Mariotti et al., 2002; Vicente-Serrano, 2005; Brönnimann, 2007; Brönnimann et al., 2007). Mariotti et al. (2002)
40 showed that precipitation decreases over the western Mediterranean during La Niña in autumn, spring. During the late winter,
Brönnimann (2007) suggested a connection between La Niña (El Niño) and the positive (negative) phase of the NAO.

The increases in the severity and number of droughts over the region have been already detected in the modern observational
records since the mid to late 20th century through different drought indices (e.g., Mariotti et al., 2008; Philandras et al.,
2011; Sousa et al., 2011; Seager et al., 2014; Vicente-Serrano et al., 2014; Spinoni et al., 2015). This increase in dryness is
45 attributed to the increase in the atmospheric greenhouse gases (GHG) concentration, which causes a strong increase in the
surface temperature and decrease in precipitation over the region. In addition, general circulation models (GCMs) project
that this drying trend together with the increases in dry days and drought episodes will be intensified in the future under the
business-as-usual scenario, causing important socio-economic impacts and changes in the region (Mariotti et al., 2008; Field
et al., 2012; Lehner et al., 2017; Naumann et al., 2018). The future changes in the Mediterranean droughts are due to the
50 tropical SST warming, expansion of the Hadley cell, and the expansion of the subtropical subsidence zones, intensification of
anticyclones, and northward shift of the storm tracks (Giorgi and Lionello, 2008; Mariotti et al., 2008; Hoerling et al., 2011;
Field et al., 2012; Dubrovský et al., 2014; Seager et al., 2014).

Though the dryness projected in the future scenarios by GCMs is unprecedentedly intense, multi-years long desiccation is
not a completely new phenomenon over the Mediterranean. Using the summer self-calibrated Palmer Drought Severity Index
55 (scPDSI) based on tree rings (also known as the Old World Drought Atlas; OWDA), Cook et al. (2015) showed that there
have been several dry periods during the last millennium over the Mediterranean, some with persistent pan-Mediterranean
characteristics. The region has also experienced droughts with frequencies of not only interannual, but decadal-to-multidecadal
timescales. Although, the causes of those droughts in the past are still unclear, they show some connection with the NAO (Cook
et al., 2016a) and the tropical volcanic eruptions (Rao et al., 2017).



60 Besides natural climate proxies, GCMs are useful tools to study long term changes and variability of global and regional hydroclimate and extreme events (PAGES Hydro2k Consortium, 2017; Haywood et al., 2019). For example, GCMs are employed to investigate the possible causes of the past South Western United States (SW) megadroughts, the decadal-to-centennial long intense droughts, and North American pan-continental droughts during the last millennium (Coats et al., 2016; Cook et al., 2016b; Coats and Karnauskas, 2017). The results show that different GCMs are able to reproduce the duration and intensity
65 of SW megadroughts during the Medieval Climate Anomaly (MCA) and North American pan-continental droughts, indicating the internal variability as the main driver of these megadroughts, though specific causing modes of variability are largely model dependent. Stevenson et al. (2018) used the Community Earth System Last Millennium Ensemble (Otto-Bliesner et al., 2016) to examine the connection between past global hydrological mega-events, and climate variability and external forcings during the last millennium. Among the major modes of climate variability, the influences of ENSO and AMO on mega-events have been
70 found, both significantly altering the megadrought risks and persistence in drought-prone regions, for instance, the southern Australia, the Sahel and the southern United States. The study provides insights into the dynamic of megadroughts associated with different mode of variability in global scale, though, a detailed analysis on southern Europe and the Mediterranean is missing.

In studies of the hydroclimate during last millennium over the European domain, Ljungqvist et al. (2019) examined the
75 long-term relationship between the warm season temperature and hydroclimate during the Common Era by using instrumental records, reconstructions, and model simulations. Their study reveals that southern Europe shows a warm-dry temperature-hydroclimate co-variability at multidecadal timescales. In particular for the Mediterranean, Xoplaki et al. (2018) investigated the interaction between the past central and eastern Mediterranean societies and the hydroclimate conditions including droughts by comparing the historical records, proxies and GCM simulations. Analyzing three specific historical multidecadal periods,
80 they concluded that the multidecadal variability of precipitation in the region is driven by internal dynamics of the climate system: large discrepancies between the model trajectories are detected. Therefore, no agreement in timing between models-proxies-historical records can be expected. Nevertheless, the models elucidate some possible explanations about the dynamics of extreme dry and wet events in some past periods.

Despite a number of studies on past hydrological variability, a long-term continuous perspective on the mechanisms of past
85 extreme hydrological events, specifically of droughts over the Mediterranean is still not fully explored. As a long trend of dryness has already been detected in the instrumental era and is expected to intensify in the future scenario, it is necessary to provide a long-term picture on the variability and changes of past dry events and their mechanisms. Therefore, we aim to examine the physical mechanisms involved in yearly and multi-year long droughts during the Common Era (850 - 1849 AD) and historical and future periods (1850 - 2099 AD) over the western and central Mediterranean. We focus on understanding
90 the dynamics that induce past persistent multi-year Mediterranean droughts, and whether the dynamics that induce droughts in the past will change in the historical and future periods with the anthropogenic increase in GHG. For our purpose, we use the Community Earth System Model version 1.0.1 (CESM), which includes the active biogeochemical cycle and has the high horizontal resolution of $1.25^\circ \times 0.9^\circ$ (Lehner et al., 2015).



This paper is composed of following sections: in section 2, we introduce the model and simulations, the hydrological variables given by the model, definition of droughts, drought indices and methods. In section 3, we present the results of our analysis: first, we describe how the model depicts the past droughts and whether the quantification of past droughts over the region is sensitive to the choice of drought metrics; second, we report the climate conditions associated with the past Mediterranean droughts and their connection with regional scale circulation and modes of variability, i.e. the NAO and ENSO; lastly, we discuss whether mechanisms that induce past droughts have changed in the historical and future periods. In section 4, we close the paper with a brief conclusion.

2 Model description and methods

2.1 Description of the model and simulations

The Community Earth System model version 1.0.1 is a fully coupled general circulation model composed of the Community Atmosphere Model version 4 for the atmosphere (Neale et al., 2010), the Community Land Model version 4 for the land (Lawrence et al., 2011), the Parallel Ocean Program version 2 for the ocean (Danabasoglu et al., 2011), and the Community Ice Code version 4 for the sea ice (Hunke et al., 2010). We use a transient simulation for the last 1150 years (850 - 2000 AD), the future 100 years with the RCP 8.5 scenario (2001 - 2099 AD), and the control simulation of 400 years at perpetual 850 AD conditions (Lehner et al., 2015). In the simulations, the atmosphere has the horizontal resolution of $1.25^\circ \times 0.9^\circ$ and 26 vertical layers, and the land has the same horizontal resolution as the atmosphere with 15 sub-surface layers. The ocean has the horizontal resolution of $1.25^\circ \times 0.9^\circ$ with displaced pole grids with 60 ocean layers.

The control simulation uses constant forcing parameters set to the 850 AD values: the land use changes, the total solar irradiance in which the value is $1360.228 \text{ W m}^{-2}$, the GHG concentration, such as the CO_2 of 279.3 ppm, CH_4 of 674.5 ppb and the N_2O of 266.9 ppb. Unlike other forcings, the orbital parameters are set to 1990 AD conditions.

The transient simulation includes the active biogeochemical cycle and forcings, such as the land use changes, total solar irradiance, volcanic eruptions and greenhouse gases concentrations that vary over time (Schmidt et al., 2012). The GHG concentrations and land use changes vary little before 1850, showing pronounced changes and increases after that year. A more detailed overview of the forcings and initial set-up of the simulations is presented in Lehner et al. (2015).

2.2 Analysis and methods

For the analysis, we split the transient simulation into two parts: the first period from 850 to 1849 AD is used to study the natural variability of droughts excluding the effect of accelerated increase in the GHGs, and the second period from 1850 to 2099 AD is used to examine the effects of anthropogenic changes on the natural variability of droughts. The drought condition during first period is compared to the control simulation to assess the influence of the natural forcings.

The statistical tests to compare the transient to the control simulations are performed with the Mann-Whitney U significance test for the means at a 5% confidence level. First, the test is performed without considering the difference in the length of each



125 simulation. Then, as the transient simulation is longer than the control one, we select 5 sets of random 89 years with droughts
from the transient simulation and apply the tests against the control simulation.

The focus area of the study is the western and central Mediterranean region confined to $15^{\circ}\text{W} - 28^{\circ}\text{E}$ and $33^{\circ} - 45^{\circ}\text{N}$ (Fig. 1). The monthly anomalies of the variables associated with the hydrological condition, such as the surface and air temperatures, precipitation, zonal and meridional winds, geopotential heights, and sea level pressure are calculated with respect to the 1000-
130 1849 AD (850 years) mean annual cycle for each grid point. For the control simulation, the entire 400 years are taken as a reference period to calculate the anomalies. The anomalies during the historical and future period (1850 - 2099 AD) are linearly detrended in order to examine the dryness during this period without the anthropogenic increase in temperature. This is carried out by applying the least squares method to the each of the periods: from 1850 to 2000 and from 2001 to 2099.

Additionally, composites of positive and negative phases of two modes of variability are investigated: the NAO and ENSO.
135 The NAO is taken as the difference in the sea level pressure anomalies between the regions confined to $33^{\circ} - 21^{\circ}\text{W} / 35^{\circ} - 39^{\circ}\text{N}$ and $25^{\circ} - 13^{\circ}\text{W} / 63^{\circ} - 67^{\circ}\text{N}$, which reflects the Azores high and the Iceland low, respectively (Wallace and Gutzler, 1981; Trigo et al., 2002). The ENSO is characterized by the annual mean sea surface temperature anomalies over Niño 3.4 region in the Tropical Equatorial Pacific ($170^{\circ} - 120^{\circ}\text{W}$ and $5^{\circ}\text{S} - 5^{\circ}\text{N}$) (Trenberth, 1997).

2.3 Drought definitions

140 We use some drought metrics to quantify droughts: the Standardized Precipitation Index (SPI), Standardized Precipitation Evapotranspiration Index (SPEI), self-calibrated Palmer Drought Severity Index (scPDSI), and annual soil moisture anomaly (SOIL).

The SPI only requires a long-term precipitation record, and the accumulated precipitation is fitted to a probabilistic distribution, in our case a gamma distribution. Then, the fitted distribution is transformed to a normalized Gaussian distribution
145 (McKee et al., 1993). The SPEI is similar to the SPI, but instead of only using a precipitation record, it considers the climate water balance given by the difference between the precipitation and atmospheric evaporative demand. This difference is fitted to a log-logistic probability distribution, then, transformed to a normal distribution (Vicente-Serrano et al., 2009). For the atmospheric evaporative demands, we use the potential evapotranspiration derived from Thornthwaite equation, which only requires surface temperature and latitude (Thornthwaite et al., 1948). The scPDSI computes the water balance by assuming a
150 two-layer soil bucket model, and it requires temperature and potential evapotranspiration records. Other necessary variables, such as runoff and losses, are estimated from the temperature and potential evapotranspiration (Palmer, 1965; Wells et al., 2004; Zhong et al., 2018). Again, the potential evapotranspiration is calculated by using Thornthwaite equation same as the SPEI. The SOIL is the upper 10 cm soil moisture anomaly calculated with respect to the 850 years-mean (1000-1849 AD) annual cycles. The soil moisture is a direct output from the model.

155 All indices are calculated with respect to the same reference period (1000-1849 AD), and with the 12 months-annual time scale for the SPI, SPEI and SOIL. The scPDSI has an inherent time scale that ranges from 9 to 14 months depending on the region (Vicente-Serrano et al., 2010, 2015). Thus, we use a 12 months time scale for the other indices in order to be comparable to the scPDSI. Then, all indices are area weighted averaged over the Mediterranean region (Fig. 1). The summer scPDSI is



also calculated as a mean of June, July and August, then, compared to the scPDSI from the OWDA, which is the $0.5^\circ \times 0.5^\circ$
160 gridded reconstruction of European summer scPDSI from tree rings (Cook et al., 2015).

For all indices, we define a drought event as consecutive years with negative indices, in which at least one year with the index
falling below the 10 percentile of its 850 year (1000 - 1849 AD) distribution. In such way, we assure that the dry condition is
maintained consistently during drought years, without being interrupted by one very wet year or season, and the dry condition
is extreme enough to be considered as a drought event.

165 Then, droughts with a duration of more than 3 years are considered as multi-year droughts. In Sect. 3.2, we analyze the mean
condition during droughts in the control and transient simulations taking into account all short (1 and 2 years of duration) and
long (more than 3 years of duration) Mediterranean droughts. For the next part of the analysis in Sect. 3.3, we examine the
dynamics associated with persistent multi-year droughts (more than 3 years of duration). These long droughts are separated
into three stages: the initiation year as the first year of drought, the termination year as the last year, and the rest as the transition
170 year. The evolution of droughts is analyzed for each of the stages.

3 Results

3.1 Quantification of drought events over the Mediterranean: Selection of a drought index

To gain an overview of drought conditions in the Mediterranean, we assess the different indices defined in Sect. 2.3 using the
period 850 to 1849 AD and focusing on the drought events and their duration. In particular, we compare the variability and
175 duration of droughts of the summertime scPDSI with those from OWDA to validate our simulations. As a comparison between
the proxies and our model simulation cannot be directly made due to the different initial conditions between the proxies and
model (PAGES Hydro2k Consortium, 2017; Xoplaki et al., 2018), we check whether the summer drought variability given by
the model is similarly represented to that of proxies, mostly in term of duration.

Fig. 2 shows that indeed, the model is able to reproduce persistent multi-year drought events, which are comparable with
180 the proxies: the number and the duration of summer droughts in the model are similar to that of the proxies with a continuous
appearance of the events over time (Fig. 2.(a) and (c)) Hence, the model is able to reproduce past multi-year Mediterranean
droughts indicating that the simulation is suitable to study the past droughts.

Annual Mediterranean droughts and their duration given by different indices are presented in Fig. 2.(b) and (d). As expected,
the different indices do not exactly behave similarly in terms of the occurrence, number of events, and duration (Raible et al.,
185 2017; Mukherjee et al., 2018). However, they still show good coherence for some periods: for 89 years of the 850 - 1849 AD
period, all indices indicate the same overlapped drought periods.

In terms of duration, the scPDSI is the one which shows more longer droughts than other indices, with a mean duration of
9.1 years (Fig. 2.(d)). Then, the SPEI, SOIL and SPI follow it with the mean durations of 2.9, 2.8, and 2.3 years, respectively.
The SPI presents more events than other indices, but with shorter duration. First, this difference in duration of droughts can be
190 attributed to the water balance variables involved in the computation of each index. For instance, the SPI only takes precipi-
tation as its input variable. Thus, it does not take into account the atmospheric evaporative demands, which can be intensified



during dry periods. Therefore, we expect that the SPI shows a reduced duration of droughts compared to the scPDSI and SPEI, which include the potential evapotranspiration in their water balance. The same holds true for the SOIL index. Though, the soil moisture variable in the model is closely connected to the hydrological cycle reflecting the balance between the precipitation and actual evapotranspiration, the magnitude of actual evapotranspiration over the region is smaller than the potential evapotranspiration derived from the Thornthwaite method. Hence, the water balance involved in SOIL is affected in such a way that the drought duration is reduced compared to the scPDSI and SPEI. Lastly, droughts with relatively longer duration in the scPDSI can be explained by the memory effect embedded in the calculation scheme of scPDSI (Palmer, 1965; Wells et al., 2004), which other indices that are obtained by being normalized with respect to certain statistical distribution families do not present. Note that the scPDSI is an accumulating index. Thus, during the calculation process, the weighted value of preceding months is used to estimate the index for the current month, implying a persistence of the events. Hence, with the scPDSI, an intense yearly drought would likely induce a drought in the following year and this effect can be exacerbated in the context of intense multi-year droughts.

In terms of variability over the period of 850 - 1849 AD, no noticeable changes, such as a sudden increase or decrease, in the occurrence of droughts over some common periods is found among the indices (Fig. 2.(b)). This gives us a first hint that the occurrence of yearly and multi-year Mediterranean droughts are not driven by the external natural forcing. Thus internal variability of the climate system and the regional climate conditions plays the dominant role in the generation of droughts.

For the next sections, we present our analysis on dynamics associated with Mediterranean droughts using the SOIL as the drought indicator. The reason is that the SOIL overlaps full or a part of drought periods given by the other three indices, without significantly underestimating the multi-year duration of droughts (Fig. 2.(b) and (d)). The droughts in SOIL overlap the 36%, 25% and 29% of droughts in the scPDSI, SPEI and SPI, respectively. Also, the SOIL and each of the indices are statistically correlated at 1% confidence level for the entire period of 850 -1849 AD with Pearson correlation coefficients of 0.81 (scPDSI), 0.78 (SPEI) and 0.86 (SPI). Thus, the results in the following sections can be transferred to the other indices. To guarantee the transferability the analysis in the next sections was repeated with each of the drought indices, showing similar results as for SOIL (therefore figures not shown).

3.2 Atmospheric circulation associated with Mediterranean droughts (850 - 1849 AD)

In this section, the atmospheric circulation associated with Mediterranean droughts is investigated by using the SOIL in the control and transient simulations up to 1849 AD. The control simulation presents 29 drought events, which are in total 89 years long, and the transient simulation has 80 drought events, covering 225 years. The difference in the numbers of events is simply due to the different lengths of the simulations.

To get a first glance of the atmospheric circulation during drought conditions, Fig. 3 presents the anomalies of geopotential height at 850 hPa and surface temperature during Mediterranean droughts for each simulation. Though both simulations differ in the total numbers of droughts, the structures of geopotential height and temperature anomalies during Mediterranean droughts are similar, with a high pressure system centered over central Europe accompanied by a positive temperature anomaly. This high pressure anomaly, which from now on is called the drought high, is found in all heights from the 850 to 300 hPa (fig-



ures not shown), indicating a barotropic nature of this atmospheric circulation system. Additionally, a low pressure anomaly is situated over the area of Scandinavia to Russia. Thus, the atmospheric circulation shows a north easterly shift of the westerlies over Europe, so that moist air masses from the North Atlantic are passed around the Mediterranean.

Outside the European continent, a negative temperature anomaly over the Tropical Equatorial Pacific and a positive anomaly
230 over the North Pacific are prominent in both simulations. These temperature patterns resemble the cold phase of ENSO and the positive phase of Pacific Decadal Oscillation (PDO), respectively. Besides, a positive geopotential height anomaly at the mid-latitudes and a negative anomaly at the high-latitudes over the North Atlantic region is another pattern that both simulations share in common during droughts. This pattern is similar to the positive phase of the NAO; however, the southerly center
235 of action is shifted to central Europe, which also resembles partially the East Atlantic Pattern (EA). The means of these common patterns are also statistically indifferent between both simulations (Fig. 3), indicating that they are derived from the same statistical populations. Thus, they share common mechanisms associated with droughts, mainly driven by the internal variability of the climate system in the model, embedded both in control and transient simulations.

The drought high is a clear feature that appears during all droughts over the region. This pattern over central Europe and the western Mediterranean is similar to the pattern of the first mode of canonical correlation described by Xoplaki et al. (2003). In
240 Xoplaki et al. (2003), this pattern is associated with the variability of temperature during the summertime in the Mediterranean region. In our study, the high pressure system is present during all seasons of years with droughts, showing a relatively stronger intensity in winter and spring compared to summer (Fig. 4). This is expected, as the variability of the geopotential height fields over Europe and the North Atlantic is reduced in summer compared to the other seasons, because of the fact that the meridional temperature gradient on the Northern Hemisphere is also reduced. Therefore, the main forcing of the atmospheric circulation
245 is weakened. Hence, our findings show that the atmospheric conditions in winter and spring are determinant at controlling the annual mean hydroclimate, indicating the importance of the winter and spring seasons in annual cycle of precipitation over the Mediterranean. In our simulation, 56% of the annual precipitation falls in the winter and spring, while the summer precipitation amounts only to 15%; similar to other studies (Lionello et al., 2006; Xoplaki et al., 2004; Zveryaev, 2004). As expected, a decrease in precipitation occurs during drought years in all seasons: the winter and spring precipitation decreases by
250 around 13%, and the summer and autumn precipitation is reduced by 11% compared to non-drought periods. The temperature shows a positive anomaly over the Mediterranean in all seasons, with strongest signals during summer and autumn, a finding which is in line with, e.g., Xoplaki et al. (2003).

3.3 Dynamics of multi-year droughts

As shown in the previous section in Fig. 3, the drought high is a prominent atmospheric circulation pattern with the negative
255 geopotential height anomaly north-east to it. The entire pattern resembles the positive NAO-like pattern, although with a shift to the North-East. At the same time, a colder than normal condition over the Tropical Equatorial Pacific is detected, which is similar to a La Niña-like condition (negative ENSO). In the following, the origin and the evolution of Mediterranean long droughts associated to the drought high is investigated using the transient simulation up to 1849 AD. The starting point is



whether the dry condition and drought high are originated from the NAO-like or ENSO-like condition, or if they are connected
260 to one or both of them.

When we consider the co-occurrence of drought years and the positive phase of the NAO, our simulation shows that droughts
occur more frequently during the positive phase of annual and winter NAO than during normal years. 62% of the drought years
show a positive phase of the annual NAO (58% for the winter; Fig. 5.(a)). However, the positive NAO condition does not persist
throughout the entire years with multi-year droughts. Rather, it fluctuates from its positive to negative phase during multi-year
265 droughts.

Assessing the co-occurrence between drought and cold Tropical Equatorial Pacific (La Niña-like) conditions, we find that
during 58% of total drought periods, La Niña-like conditions are also present (Fig. 5.(a)). Tropical Equatorial SSTs below -0.5°
C are found during 39% of the drought years, while the SST is above 0.5° C in 21% of the total drought periods. Thus, similar
to the findings of the NAO, La Niña-like conditions do not persist throughout the entire drought years.

270 To examine the behavior of the atmosphere during multi-years Mediterranean droughts, the frequency of modes of variability
and mean composites of circulation during droughts are split in three stages (Sect. 2.3). The positive NAO and La Niña-like
condition occur more frequently in the initiation year than the transition years or the termination year of droughts (Fig.5.(b)).
The positive NAO presents 77% and La Niña-like condition 60% of occurrence during the initiation year. These patterns
decrease in occurrence throughout the development of droughts, with 57% and 55% in the transition years, and 54% and 40%
275 in the termination year.

The specific humidity, temperature, and winds at 925 hPa level during Mediterranean droughts with a positive phase of
the NAO in the initiation year is presented in Fig. 6. During the initiation year, the southerly winds prevail over the southern
Mediterranean and weak westerlies dominate the north-west Africa and eastern North Atlantic region. The southerlies block
the intrusion of the westerly systems from the North Atlantic, and together with the cyclonic winds in the East Atlantic advect
280 dry and warm air masses from the East Atlantic and the southern Mediterranean to the continent. During the transition years,
the complete anticyclonic circulation associated with the high over central Europe and the Mediterranean region is developed.
This anticyclonic system distributes the warm and dry air to the north of the continent and sustains a dryness over the region,
therefore, initiating a long drought and enlarging its duration. During these years, the westerlies from the North Atlantic are
clearly weakened. In the termination year, a clear change in the direction of winds over Europe is observed, which indicates a
285 break-up of the high. The winds become weaker over southern Europe and easterlies occupy the northern sector. The intensities
of specific humidity and temperature anomalies are also reduced compared to the previous stages.

The mean condition during droughts with La Niña-like in the initiation year is presented in the Fig. 7. The composites of
specific humidity, temperature, and winds during the initiation years resemble those during the positive NAO, with warm and
dry air over the northern Africa and eastern North Atlantic sector, and with the westerlies from the North Atlantic that distribute
290 this air mass to the continent. Similar to Fig.6, the anticyclonic circulation associated with the drought high is also developed
during the transition years spreading the south-eastern air mass to the entire continent. The break-up of this system appears
in the termination years with the dominance of easterlies over the Mediterranean region and weakening of the humidity and
temperature anomalies.



The analysis of modes of variability during droughts shows that the combination of NAO and La Niña-like condition is important in the initiation year of Mediterranean droughts, as they provide helpful dry condition during the early stage of the events. However, these modes of variability may not play an important role to support the perseverance of long droughts. For the transition years and termination year, other processes must be involved to sustain the dry condition.

A possible candidate of an important process for the transition stage of Mediterranean droughts is the interaction among regional atmospheric and soil variables (Fig. 8). A decrease in precipitation, supported by the positive NAO and/or La Niña-like, causes an initial regional dryness that increases the regional temperature and geopotential height. The positive temperature anomaly (TS) together with the strong positive geopotential height anomaly (GP) induce a stable atmospheric condition over the region, decreasing soil moisture (SOIL) and evapotranspiration (EV). The latter increases sensible heat (SH) and decreases latent heat (LH) fluxes during the initiation year. During the transition years, due to the stable atmospheric condition that still persists (positive GP) and the increase in SH and loss of LH in the previous stage, TS is even magnified. The TS in turn again decreases SOIL due to the increase in SH, and decreases EV and LH. Throughout droughts, the complete high is developed and persists, fueling again this positive temperature - soil moisture feedback mechanism (Seneviratne et al., 2010; Yin et al., 2014). This mechanism continues until the termination year. During the termination year, the positive GP and TS still prevail over the region, though, with reduced anomalies. Also, the magnitudes of other variables are comparably reduced compared to the previous two stages. Additionally, it is also observed that these atmospheric and soil variables during droughts clearly differ from those during non-drought situations where all show completely opposite signs.

This result indicates that once the drought high is developed, the temperature - soil moisture feedback is a more important mechanism than the connection to NAO-like and La Niña-like patterns in order to sustain the depletion of soil moisture, which means the longevity of droughts. The large circulation patterns help to support the regional dry conditions but after the initiation year, their role in sustenance of droughts are diminished.

3.4 Historical and Future condition on droughts: 1850 to 2099 AD

Here, the historical and future behavior of Mediterranean droughts as well as the associated mechanisms are analyzed. To obtain an overview, we present the time series of the drought index SOIL and precipitation anomaly (with respect to the mean of the period 1000 -1849 AD) over the Mediterranean region for the period 1850 - 2099 AD (Fig. 9). The simulation indicates that the region becomes drier for the period 1850 -2099 AD than the past, which is reflected in pronounced decreases in SOIL and precipitation. The reduction in these two variables is already noticeable from the beginning of 1850 AD concomitantly with the anthropogenic increase in GHG. By the end of the 21st century, the region experiences a constant drought situation without any wet anomaly with respect to the 1000 - 1849 AD condition. This indicates a shift of the mean climate of the region to a drier climate under the RCP 8.5 scenario, which is in line with other previous studies on the future projection of the region (e.g., Dubrovský et al., 2014; Naumann et al., 2018).

Next, we analyze whether the mechanisms associated with Mediterranean droughts presented in the previous sections have changed during this period. Previously, it was shown that past Mediterranean droughts are characterized by intense positive geopotential height and temperature anomalies over central Europe and the Mediterranean. These features are also observed



in the non-detrended 1850 - 2099 AD condition, but with more intensified positive geopotential height (GP) and temperature (TS) anomalies than during the period 850 - 1849 AD (Fig. 10.(a)). The variances of GP, TS and SOIL are enlarged; therefore, their medians and extreme tails are also magnified, which implies that the dryness and its associated atmospheric conditions become more frequent and severe in the 1850 - 2099 AD period. The increases in GP and TS clearly intensify the above-mentioned interaction among regional atmospheric and soil variables, i.e the positive temperature – soil moisture feedback. This intensification aids the longevity and intensity of droughts, which is also reflected as a reduction in the surface soil moisture anomaly (Fig. 9). Additionally, the precipitation - soil moisture interaction is involved, i.e. a continuous reduction in precipitation decreases soil moisture, thus, inducing less evapotranspiration, which leads again to a reduction in precipitation (Seneviratne et al., 2010).

Related to the large circulation patterns, the frequencies of positive NAO and La Niña-like conditions during droughts also seem to be affected by the overall change in global temperature (Fig. 10.(b)). Compared to 850 – 1849 AD, the non-detrended 1850 – 2099 AD period shows a slight reduction in the preference toward the positive NAO and La Niña-like conditions during droughts. This result is in line with the previously mentioned regional circulation conditions during droughts: in this situation where the regional atmospheric variables have a more dominant role in the regional desiccation aided by the intense GP and TS, the importance of modes of variability is reduced, even during the initial stages of droughts. Hence, non significant role of positive NAO and La Niña-like during different stages of droughts can be expected.

To see the background atmospheric condition without the effect of the increase in GHG during drought periods for 1850 – 2099 AD, the variables in which the trends were eliminated are shown in Fig. 10 and 11. The variances and means of the detrended TS, GP and SOIL are statistically indifferent to the 850-1849 AD values. The same is also true for the NAO and ENSO-like states during droughts (Fig. 10). The mean composites of detrended surface temperature and geopotential height at 850 hPa during Mediterranean droughts (Fig. 11) also supports this indifference between these two periods, exhibiting the circulation patterns during droughts which are similar to those during the 850 - 1849 AD period (Fig. 3.(a) and (b)). This result indicates that the future change in dryness and droughts over the region is undoubtedly caused by the anthropogenic increase in GHG and its influence on climate. The regional feedback associated with droughts still remains the same, though the intensity of it is magnified, and it becomes the dominant one at controlling the desiccation over the region.

4 Conclusions

We have analyzed the variability and mechanisms of multi-years droughts over the western and central Mediterranean region for the period of 850 - 1849 AD and whether these mechanisms associated with Mediterranean droughts have changed after the pre-industrial period from 1850 to 2099 AD with the anthropogenic increase in GHG. We have done this by using CESM simulations.

First of all, our analysis shows that the overall similarities in drought periods exist among indices, though, the quantification of droughts is sensitive to the choice of drought index even in the paleoclimate context. For example, in general, the scPDSI exhibits longer drought events than other indices, while the SPI is opposite, presenting more shorter events. Though, the



major mechanisms that induce multi-years droughts over the region remain similar due to the same overlapping periods and high correlation among indices, this discrepancy among indices can lead to a different conclusion, mostly in the number and duration of past drought events. This shows that using just one unique index is still complicated, even in the paleoclimate context. Hence, the uncertainty associated with different indices must be taken into account when comparing indices in drought studies (Dai, 2011; Raible et al., 2017; Mukherjee et al., 2018), in particular, in the case when only a single drought index is used and the focus is on the assessment of the duration of extreme hydrological events in past periods.

Secondly, we found that the past Mediterranean droughts are mainly induced by the internal dynamics of climate system supporting the finding of Xoplaki et al. (2018): the patterns of surface temperature and circulation over the Mediterranean during droughts in the control simulation is statistically indifferent from those of the transient simulation with full external forcing. One of the distinct patterns found during Mediterranean droughts is a barotropic high pressure system accompanied by a positive temperature anomaly over central Europe and the Mediterranean region. This warm high persists during all seasons when droughts occur over the region, showing stronger intensity during winter and spring. This result emphasizes the importance of the wet cold seasons, i.e. winter and spring climate and circulation in Mediterranean droughts. Other patterns during droughts are the positive NAO and the cold Tropical Equatorial Pacific (La Niña-like). We found that these large scale circulation patterns play a more important role during the early stage of droughts, by providing dry condition over the western and central Mediterranean region to initiate such events. Then, the longevity of droughts is determined by the interaction of regional circulation variables, which involve stable atmospheric conditions (persistence of the high pressure system), a temperature increase, changes in evapotranspiration and surface heat fluxes. Namely, this is the temperature - soil moisture feedback, which continues until the termination of droughts. During these transition years of droughts, the role played by the large-scale patterns is reduced.

Thirdly, the decreases in soil moisture and precipitation anomalies are already detected since the pre-industrial period concomitantly with the anthropogenic increase in GHG. This means that the intensification of droughts and the shift of the mean climate over the region to a drier climate have started earlier than reported in the modern observational era. This regional desiccation is principally caused by the anthropogenic increase in GHG, which induces the intensification of interactions between the regional atmospheric and soil variables, associated with the temperature- soil moisture and precipitation - soil moisture feedbacks. If the increase in temperature and decreases in precipitation continue, intensifying the depletion of soil moisture in the future, the region will suffer from a continuous desiccation instead of droughts, as droughts are the deviation from the mean hydrological condition.

Lastly, it is important to mention that our analysis is based on a single model output and this raises questions related to single model studies, such as boundary condition problems and model-dependent biases and physics (PAGES Hydro2k Consortium, 2017). Nevertheless, the study presented provides a useful understanding on long-term variability and mechanisms of droughts by analyzing the entire last millennium. We addressed distinct different roles of the large scale modes of variability and regional circulation during the different stages of multi-year droughts. In addition, we emphasized the importance of assessing different drought indices even in the paleoclimate context, and the role of the cold season in Mediterranean droughts. As the Mediterranean region is considered as one of the most vulnerable region under the current climate change scenario (Giorgi



and Lionello, 2008; Lehner et al., 2017), more studies on the topics related to droughts and permanent future desiccation are necessary to develop a better preparedness for upcoming changes.

Code availability. Two R packages were used to calculate the drought indices: the *scPDSI* (Zhong et al., 2018) and the *SPEI* (Vicente-Serrano et al., 2009)

400 *Data availability.* The summer *scPDSI* from the Old World Drought Atlas is available on: <https://www.ncdc.noaa.gov/paleo-search/study/19419> (Cook et al., 2015). The CESM simulations are available on request at the University of Bern.

Author contributions. WK and CR discussed and set up the initial research idea. WK performed the analysis and drafted the manuscript under the supervision of CR. CR provided critical feedback on the results and the manuscript. Both authors contributed to the interpretation and discussion of the results and edited the manuscript together.

405 *Competing interests.* The authors declare that they have no conflict of interest.

Acknowledgements. The study is funded by the Swiss National Science Foundation (SNSF, grant 200020_172745). We acknowledge that some simulations were performed at the Swiss National Super Computing Centre (CSCS). We thank Dr. Craig Hamilton for proofreading this manuscript.



References

- 410 Barnston, A. G. and Livezey, R. E.: Classification, seasonality and persistence of low-frequency atmospheric circulation patterns, *Monthly weather review*, 115, 1083–1126, [https://doi.org/10.1175/1520-0493\(1987\)115<1083:CSAPOL>2.0.CO;2](https://doi.org/10.1175/1520-0493(1987)115<1083:CSAPOL>2.0.CO;2), 1987.
- Brönnimann, S.: Impact of El Niño–southern oscillation on European climate, *Reviews of Geophysics*, 45, <https://doi.org/10.1029/2006RG000199>, 2007.
- Brönnimann, S., Xoplaki, E., Casty, C., Pauling, A., and Luterbacher, J.: ENSO influence on Europe during the last centuries, *Climate Dynamics*, 28, 181–197, <https://doi.org/10.1007/s00382-006-0175-z>, 2007.
- 415 Coats, S. and Karnauskas, K.: Are simulated and observed twentieth century tropical Pacific sea surface temperature trends significant relative to internal variability?, *Geophysical Research Letters*, 44, 9928–9937, <https://doi.org/10.1002/2017GL074622>, 2017.
- Coats, S., Smerdon, J. E., Cook, B., Seager, R., Cook, E. R., and Anchukaitis, K. J.: Internal ocean-atmosphere variability drives megadroughts in Western North America, *Geophysical research letters*, 43, 9886–9894, <https://doi.org/10.1002/2016GL070105>, 2016.
- 420 Cook, B. I., Anchukaitis, K. J., Touchan, R., Meko, D. M., and Cook, E. R.: Spatiotemporal drought variability in the Mediterranean over the last 900 years, *Journal of Geophysical Research: Atmospheres*, 121, 2060–2074, <https://doi.org/10.1002/2015JD023929>, 2016a.
- Cook, B. I., Cook, E. R., Smerdon, J. E., Seager, R., Williams, A. P., Coats, S., Stahle, D. W., and Díaz, J. V.: North American megadroughts in the Common Era: Reconstructions and simulations, *Wiley Interdisciplinary Reviews: Climate Change*, 7, 411–432, <https://doi.org/10.1002/wcc.394>, 2016b.
- 425 Cook, E. R., Seager, R., Kushnir, Y., Briffa, K. R., Büntgen, U., Frank, D., Krusic, P. J., Tegel, W., van der Schrier, G., Andreu-Hayles, L., et al.: Old World megadroughts and pluvials during the Common Era, *Science advances*, 1, e1500561, <https://doi.org/10.1126/sciadv.1500561>, 2015.
- Dai, A.: Drought under global warming: a review, *Wiley Interdisciplinary Reviews: Climate Change*, 2, 45–65, <https://doi.org/10.1002/wcc.81>, 2011.
- 430 Dai, A.: Increasing drought under global warming in observations and models, *Nature climate change*, 3, 52–58, <https://doi.org/10.1038/nclimate1633>, 2013.
- Danabasoglu, G., Bates, S. C., Briegleb, B. P., Jayne, S. R., Jochum, M., Large, W. G., Peacock, S., and Yeager, S. G.: The CCSM4 Ocean Component, *Journal of Climate*, 25, 1361–1389, <https://doi.org/10.1175/JCLI-D-11-00091.1>, 2011.
- Dubrovský, M., Hayes, M., Duce, P., Trnka, M., Svoboda, M., and Zara, P.: Multi-GCM projections of future drought and climate variability indicators for the Mediterranean region, *Regional Environmental Change*, 14, 1907–1919, <https://doi.org/10.1007/s10113-013-0562-z>, 2014.
- 435 Field, C. B., Barros, V., Stocker, T. F., and Dahe, Q.: Managing the risks of extreme events and disasters to advance climate change adaptation: special report of the intergovernmental panel on climate change, Cambridge University Press, 2012.
- Giorgi, F.: Climate change hot-spots, *Geophysical research letters*, 33, <https://doi.org/10.1029/2006GL025734>, 2006.
- 440 Giorgi, F. and Lionello, P.: Climate change projections for the Mediterranean region, *Global and Planetary Change*, 63, 90–104, <https://doi.org/10.1016/j.gloplacha.2007.09.005>, 2008.
- Haywood, A. M., Valdes, P. J., Aze, T., Barlow, N., Burke, A., Dolan, A. M., von der Heydt, A. S., Hill, D. J., Jamieson, S. S. R., Otto-Bliesner, B. L., Salzmann, U., Saupe, E., and Voss, J.: What can Palaeoclimate Modelling do for you?, *Earth Systems and Environment*, 3, 1–18, <https://doi.org/10.1007/s41748-019-00093-1>, 2019.



- 445 Hoerling, M., Eischeid, J., Perlwitz, J., Quan, X., Zhang, T., and Pegion, P.: On the Increased Frequency of Mediterranean Drought, *Journal of Climate*, 25, 2146–2161, <https://doi.org/10.1175/JCLI-D-11-00296.1>, 2011.
- Hunke, E. C., Lipscomb, W. H., Turner, A. K., Jeffery, N., and Elliott, S.: CICE: the Los Alamos Sea Ice Model Documentation and Software User's Manual Version 4.1 LA-CC-06-012, T-3 Fluid Dynamics Group, Los Alamos National Laboratory, 675, 2010.
- Hurrell, J. W.: Decadal trends in the North Atlantic Oscillation: regional temperatures and precipitation, *Science*, 269, 676–679, <https://doi.org/10.1126/science.269.5224.676>, 1995.
- 450 Krichak, S. O. and Alpert, P.: Decadal trends in the east Atlantic–west Russia pattern and Mediterranean precipitation, *International journal of climatology: a journal of the Royal Meteorological Society*, 25, 183–192, <https://doi.org/10.1002/joc.1124>, 2005.
- Lawrence, D. M., Oleson, K. W., Flanner, M. G., Thornton, P. E., Swenson, S. C., Lawrence, P. J., Zeng, X., Yang, Z.-L., Levis, S., Sakaguchi, K., et al.: Parameterization improvements and functional and structural advances in version 4 of the Community Land Model, *Journal of Advances in Modeling Earth Systems*, 3, <https://doi.org/10.1029/2011MS00045>, 2011.
- 455 Lehner, F., Joos, F., Raible, C. C., Mignot, J., Born, A., Keller, K. M., and Stocker, T. F.: Climate and carbon cycle dynamics in a CESM simulation from 850 to 2100 CE, *Earth System Dynamics*, 6, 411–434, <https://doi.org/10.5194/esd-6-411-2015>, 2015.
- Lehner, F., Coats, S., Stocker, T. F., Pendergrass, A. G., Sanderson, B. M., Raible, C. C., and Smerdon, J. E.: Projected drought risk in 1.5°C and 2°C warmer climates, *Geophysical Research Letters*, 44, 7419–7428, <https://doi.org/10.1002/2017GL074117>, 2017.
- 460 Lionello, P., Malanotte-Rizzoli, P., Boscolo, R., Alpert, P., Artale, V., Li, L., Luterbacher, J., May, W., Trigo, R., Tsimplis, M., Ulbrich, U., and Xoplaki, E.: The Mediterranean climate: An overview of the main characteristics and issues, in: *Developments in Earth and Environmental Sciences*, edited by Lionello, P., Malanotte-Rizzoli, P., and Boscolo, R., vol. 4 of *Mediterranean*, pp. 1–26, Elsevier, [https://doi.org/10.1016/S1571-9197\(06\)80003-0](https://doi.org/10.1016/S1571-9197(06)80003-0), 2006.
- Liu, W., Sun, F., Lim, W. H., Zhang, J., Wang, H., Shiogama, H., and Zhang, Y.: Global drought and severe drought-affected populations in 1.5 and 2 C warmer worlds, *Earth System Dynamics*, 9, 267, <https://doi.org/10.5194/esd-9-267-2018>, 2018.
- 465 Ljungqvist, F. C., Seim, A., Krusic, P. J., González-Rouco, J. F., Werner, J. P., Cook, E. R., Zorita, E., Luterbacher, J., Xoplaki, E., Destouni, G., García-Bustamante, E., Aguilar, C. A. M., Seftigen, K., Wang, J., Gagen, M. H., Esper, J., Solomina, O., Fleitmann, D., and Büntgen, U.: European warm-season temperature and hydroclimate since 850 CE, *Environmental Research Letters*, 14, 084015, <https://doi.org/10.1088/1748-9326/ab2c7e>, 2019.
- 470 Lloyd-Hughes, B.: The impracticality of a universal drought definition, *Theoretical and Applied Climatology*, 117, 607–611, <https://doi.org/10.1007/s00704-013-1025-7>, 2014.
- Mariotti, A., Zeng, N., and Lau, K.-M.: Euro-Mediterranean rainfall and ENSO—a seasonally varying relationship, *Geophysical research letters*, 29, 59–1, <https://doi.org/10.1029/2001GL014248>, 2002.
- Mariotti, A., Zeng, N., Yoon, J.-H., Artale, V., Navarra, A., Alpert, P., and Li, L. Z.: Mediterranean water cycle changes: transition to drier 21st century conditions in observations and CMIP3 simulations, *Environmental Research Letters*, 3, 044001, <https://doi.org/10.1088/1748-9326/3/4/044001>, 2008.
- 475 McKee, T. B., Doesken, N. J., Kleist, J., et al.: The relationship of drought frequency and duration to time scales, in: *Proceedings of the 8th Conference on Applied Climatology*, vol. 17, pp. 179–183, American Meteorological Society Boston, MA, 1993.
- Mishra, A. K. and Singh, V. P.: A review of drought concepts, *Journal of Hydrology*, 391, 202–216, <https://doi.org/10.1016/j.jhydrol.2010.07.012>, 2010.
- 480 Mukherjee, S., Mishra, A., and Trenberth, K. E.: Climate Change and Drought: a Perspective on Drought Indices, *Current Climate Change Reports*, 4, 145–163, <https://doi.org/10.1007/s40641-018-0098-x>, 2018.



- Naumann, G., Alfieri, L., Wyser, K., Mentaschi, L., Betts, R., Carrao, H., Spinoni, J., Vogt, J., and Feyen, L.: Global changes in drought conditions under different levels of warming, *Geophysical Research Letters*, 45, 3285–3296, <https://doi.org/10.1002/2017GL076521>, 2018.
- 485
- Neale, R. B., Chen, C.-C., Gettelman, A., Lauritzen, P. H., Park, S., Williamson, D. L., Conley, A. J., Garcia, R., Kinnison, D., Lamarque, J.-F., et al.: Description of the NCAR community atmosphere model (CAM 4.0), NCAR Tech. Note NCAR/TN-486+ STR, 1, 212, 2010.
- Otto-Bliesner, B. L., Brady, E. C., Fasullo, J., Jahn, A., Landrum, L., Stevenson, S., Rosenbloom, N., Mai, A., and Strand, G.: Climate variability and change since 850 CE: An ensemble approach with the Community Earth System Model, *Bulletin of the American Meteorological Society*, 97, 735–754, <https://doi.org/10.1175/BAMS-D-14-00233.1>, 2016.
- 490
- PAGES Hydro2k Consortium: Comparing proxy and model estimates of hydroclimate variability and change over the Common Era. *Clim Past* 13: 1851–1900, <https://doi.org/10.5194/cp-13-1851-2017>, 2017.
- Palmer, W. C.: *Meteorological drought*, vol. 30, US Department of Commerce, Weather Bureau, 1965.
- Philandras, C., Nastos, P., Kapsomenakis, J., Douvis, K., Tselioudis, G., and Zerefos, C.: Long term precipitation trends and variability within the Mediterranean region, *Natural Hazards and Earth System Sciences*, 11, 3235, <https://doi.org/10.5194/nhess-11-3235-2011>, 2011.
- 495
- Raible, C. C., Bärenbold, O., and Gómez-navarro, J. J.: Drought indices revisited – improving and testing of drought indices in a simulation of the last two millennia for Europe, *Tellus A: Dynamic Meteorology and Oceanography*, 69, 1287–1292, <https://doi.org/10.1080/16000870.2017.1296226>, 2017.
- Rao, M. P., Cook, B. I., Cook, E. R., D’Arrigo, R. D., Krusic, P. J., Anchukaitis, K. J., LeGrande, A. N., Buckley, B. M., Davi, N. K., Leland, C., and Griffin, K. L.: European and Mediterranean hydroclimate responses to tropical volcanic forcing over the last millennium, *Geophysical Research Letters*, 44, 5104–5112, <https://doi.org/10.1002/2017GL073057>, 2017.
- 500
- Schmidt, G. A., Jungclaus, J. H., Ammann, C. M., Bard, E., Braconnot, P., Crowley, T. J., Delaygue, G., Joos, F., Krivova, N. A., Muscheler, R., Otto-Bliesner, B. L., Pongratz, J., Shindell, D. T., Solanki, S. K., Steinhilber, F., and Vieira, L. E. A.: Climate forcing reconstructions for use in PMIP simulations of the Last Millennium (v1.1), *Geoscientific Model Development*, pp. 185–191, <https://doi.org/10.5194/gmd-5-185-2012>, 2012.
- 505
- Seager, R., Liu, H., Henderson, N., Simpson, I., Kelley, C., Shaw, T., Kushnir, Y., and Ting, M.: Causes of Increasing Aridification of the Mediterranean Region in Response to Rising Greenhouse Gases, *Journal of Climate*, 27, 4655–4676, <https://doi.org/10.1175/JCLI-D-13-00446.1>, 2014.
- Seneviratne, S. I., Corti, T., Davin, E. L., Hirschi, M., Jaeger, E. B., Lehner, I., Orlowsky, B., and Teuling, A. J.: Investigating soil moisture–climate interactions in a changing climate: A review, *Earth-Science Reviews*, 99, 125–161, <https://doi.org/10.1016/j.earscirev.2010.02.004>, 2010.
- 510
- Sousa, P. M., Trigo, R. M., Aizpurua, P., Nieto, R., Gimeno, L., and Garcia-Herrera, R.: Trends and extremes of drought indices throughout the 20th century in the Mediterranean, *Natural Hazards and Earth System Sciences*, 11, 33–51, <https://doi.org/10.5194/nhess-11-33-2011>, 2011.
- 515
- Spinoni, J., Naumann, G., Vogt, J. V., and Barbosa, P.: The biggest drought events in Europe from 1950 to 2012, *Journal of Hydrology: Regional Studies*, 3, 509–524, <https://doi.org/10.1016/j.ejrh.2015.01.001>, 2015.
- Stevenson, S., Overpeck, J. T., Fasullo, J., Coats, S., Parsons, L., Otto-Bliesner, B., Ault, T., Loope, G., and Cole, J.: Climate variability, volcanic forcing, and last millennium hydroclimate extremes, *Journal of Climate*, 31, 4309–4327, <https://doi.org/10.1175/JCLI-D-17-0407.1>, 2018.



- 520 Thornthwaite, C. W. et al.: An approach toward a rational classification of climate, *Geographical review*, 38, 55–94,
<https://doi.org/10.2307/210739>, 1948.
- Trenberth, K. E.: The Definition of El Niño, *Bulletin of the American Meteorological Society*, 78, 2771–2778, [https://doi.org/10.1175/1520-0477\(1997\)078<2771:TDOENO>2.0.CO;2](https://doi.org/10.1175/1520-0477(1997)078<2771:TDOENO>2.0.CO;2), 1997.
- Trigo, R., Osborn, T., and Corte-Real, J.: The North Atlantic Oscillation influence on Europe: climate impacts and associated physical
525 mechanisms, *Climate Research*, 20, 9–17, <https://doi.org/10.3354/cr020009>, 2002.
- Ulbrich, U. and Christoph, M.: A shift of the NAO and increasing storm track activity over Europe due to anthropogenic greenhouse gas
forcing, *Climate dynamics*, 15, 551–559, <https://doi.org/10.1007/s003820050299>, 1999.
- Vicente-Serrano, S. M.: El Niño and La Niña influence on droughts at different timescales in the Iberian Peninsula, *Water Resources Research*,
41, <https://doi.org/10.1029/2004WR003908>, 2005.
- 530 Vicente-Serrano, S. M., Beguería, S., and López-Moreno, J. I.: A Multiscalar Drought Index Sensitive to Global Warming: The Standardized
Precipitation Evapotranspiration Index, *Journal of Climate*, 23, 1696–1718, <https://doi.org/10.1175/2009JCLI2909.1>, 2009.
- Vicente-Serrano, S. M., Beguería, S., López-Moreno, J. I., Angulo, M., and El Kenawy, A.: A new global 0.5 gridded dataset (1901–2006)
of a multiscalar drought index: comparison with current drought index datasets based on the Palmer Drought Severity Index, *Journal of
Hydrometeorology*, 11, 1033–1043, <https://doi.org/10.1175/2010JHM1224.1>, 2010.
- 535 Vicente-Serrano, S. M., Lopez-Moreno, J.-I., Beguería, S., Lorenzo-Lacruz, J., Arturo Sanchez-Lorenzo, García-Ruiz, J. M., Azorin-Molina,
C., Morán-Tejeda, E., Revuelto, J., Ricardo Trigo, Coelho, F., and Espejo, F.: Evidence of increasing drought severity caused by tempera-
ture rise in southern Europe, *Environmental Research Letters*, 9, 044 001, <https://doi.org/10.1088/1748-9326/9/4/044001>, 2014.
- Vicente-Serrano, S. M., Van der Schrier, G., Beguería, S., Azorin-Molina, C., and Lopez-Moreno, J.-I.: Contribution of pre-
cipitation and reference evapotranspiration to drought indices under different climates, *Journal of Hydrology*, 526, 42–54,
540 <https://doi.org/10.1016/j.jhydrol.2014.11.025>, 2015.
- Wallace, J. M. and Gutzler, D. S.: Teleconnections in the Geopotential Height Field during the Northern Hemisphere Winter, *Monthly
Weather Review*, 109, 784–812, [https://doi.org/10.1175/1520-0493\(1981\)109<0784:TITGHF>2.0.CO;2](https://doi.org/10.1175/1520-0493(1981)109<0784:TITGHF>2.0.CO;2), 1981.
- Wells, N., Goddard, S., and Hayes, M. J.: A Self-Calibrating Palmer Drought Severity Index, *Journal of Climate*, 17, 2335–2351,
[https://doi.org/10.1175/1520-0442\(2004\)017<2335:ASPDSI>2.0.CO;2](https://doi.org/10.1175/1520-0442(2004)017<2335:ASPDSI>2.0.CO;2), 2004.
- 545 Willite, D.: Understanding the Phenomenon of Drought, Drought Mitigation Center Faculty Publications, <https://digitalcommons.unl.edu/droughtfacpub/50>, 1993.
- Xoplaki, E., González-Rouco, J. F., Luterbacher, J., and Wanner, H.: Mediterranean summer air temperature variability and its connection to
the large-scale atmospheric circulation and SSTs, *Climate Dynamics*, 20, 723–739, <https://doi.org/10.1007/s00382-003-0304-x>, 2003.
- Xoplaki, E., González-Rouco, J., Luterbacher, J., and Wanner, H.: Wet season Mediterranean precipitation variability: influence of large-scale
550 dynamics and trends, *Climate dynamics*, 23, 63–78, 2004.
- Xoplaki, E., Luterbacher, J., Wagner, S., Zorita, E., Fleitmann, D., Preiser-Kapeller, J., Sargent, A. M., White, S., Toreti, A., Haldon, J. F.,
Mordechai, L., Bozkurt, D., Akçer-Ön, S., and Izdebski, A.: Modelling Climate and Societal Resilience in the Eastern Mediterranean in
the Last Millennium, *Human Ecology*, 46, 363–379, <https://doi.org/10.1007/s10745-018-9995-9>, 2018.
- Yin, D., Roderick, M. L., Leech, G., Sun, F., and Huang, Y.: The contribution of reduction in evaporative cooling to higher surface air
555 temperatures during drought, *Geophysical Research Letters*, 41, 7891–7897, <https://doi.org/10.1002/2014GL062039>, 2014.
- Zhong, R., Chen, X., Wang, Z., and Lai, C.: scPDSI: Calculation of the Conventional and Self-Calibrating Palmer Drought Severity Index,
<https://CRAN.R-project.org/package=scPDSI>, r package version 0.1.3, 2018.

<https://doi.org/10.5194/cp-2020-79>
Preprint. Discussion started: 6 July 2020
© Author(s) 2020. CC BY 4.0 License.



Zveryaev, I. I.: Seasonality in precipitation variability over Europe, *Journal of Geophysical Research: Atmospheres*, 109, <https://doi.org/10.1029/2003JD003668>, 2004.

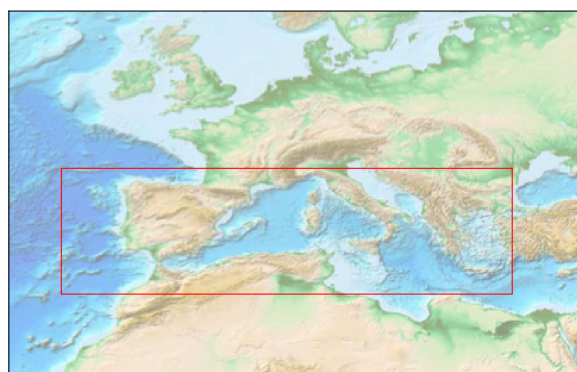


Figure 1. Region of study: the western and central Mediterranean.

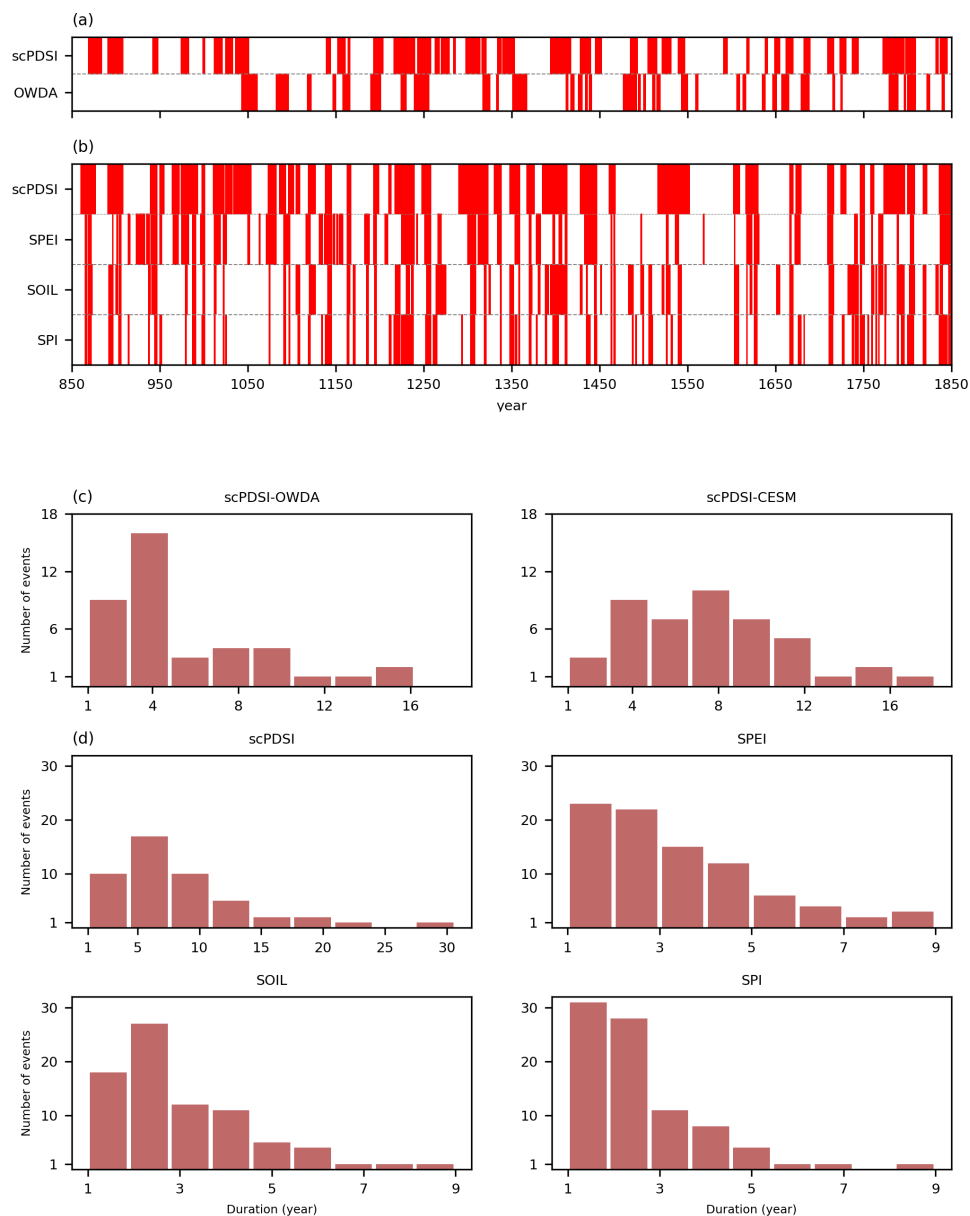


Figure 2. Occurrence of Mediterranean droughts from 850 to 1849 AD given by different drought indices: (a) Mean June-July-August (summer) indices, (b) annual indices, (c) the histograms of duration and number of droughts for the summer, and (d) annual indices. The indices are annual soil moisture anomaly (SOIL), Standardized Precipitation Evapotranspiration Index (SPEI), Standardized Precipitation Index (SPI), self-calibrated Palmer Drought Severity Index (scPDSI) calculated from the transient simulation, and the self-calibrated Palmer Drought Severity Index from tree ring proxies in Old World Drought Atlas (OWDA). Note that on (d), the scPDSI is drawn with different values of duration to other indices.

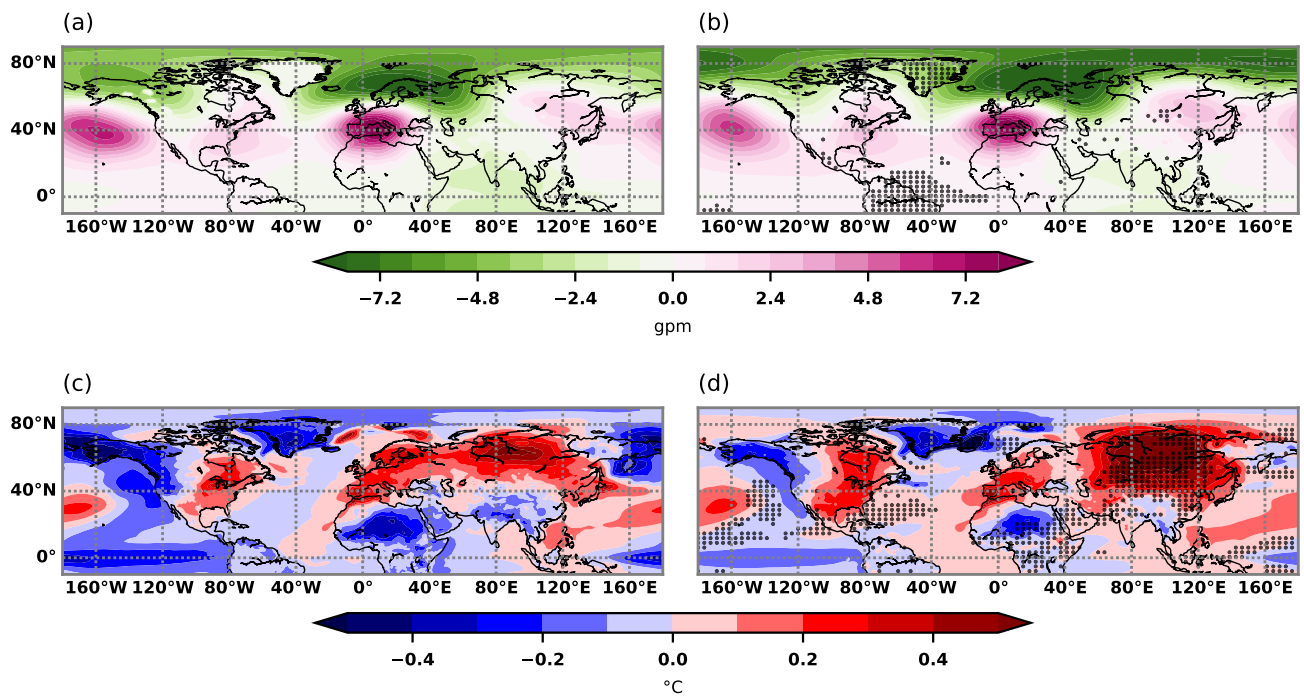


Figure 3. (Above) Mean geopotential height anomaly at 850hpa, and (below) mean surface temperature anomaly, for the (a) and (c) control, (b) and (d) transient simulations during Mediterranean droughts. Black dots in the transient simulation (b) and (d) indicate the regions where the means are not statistically significant at 5% confidence level to the control simulation.

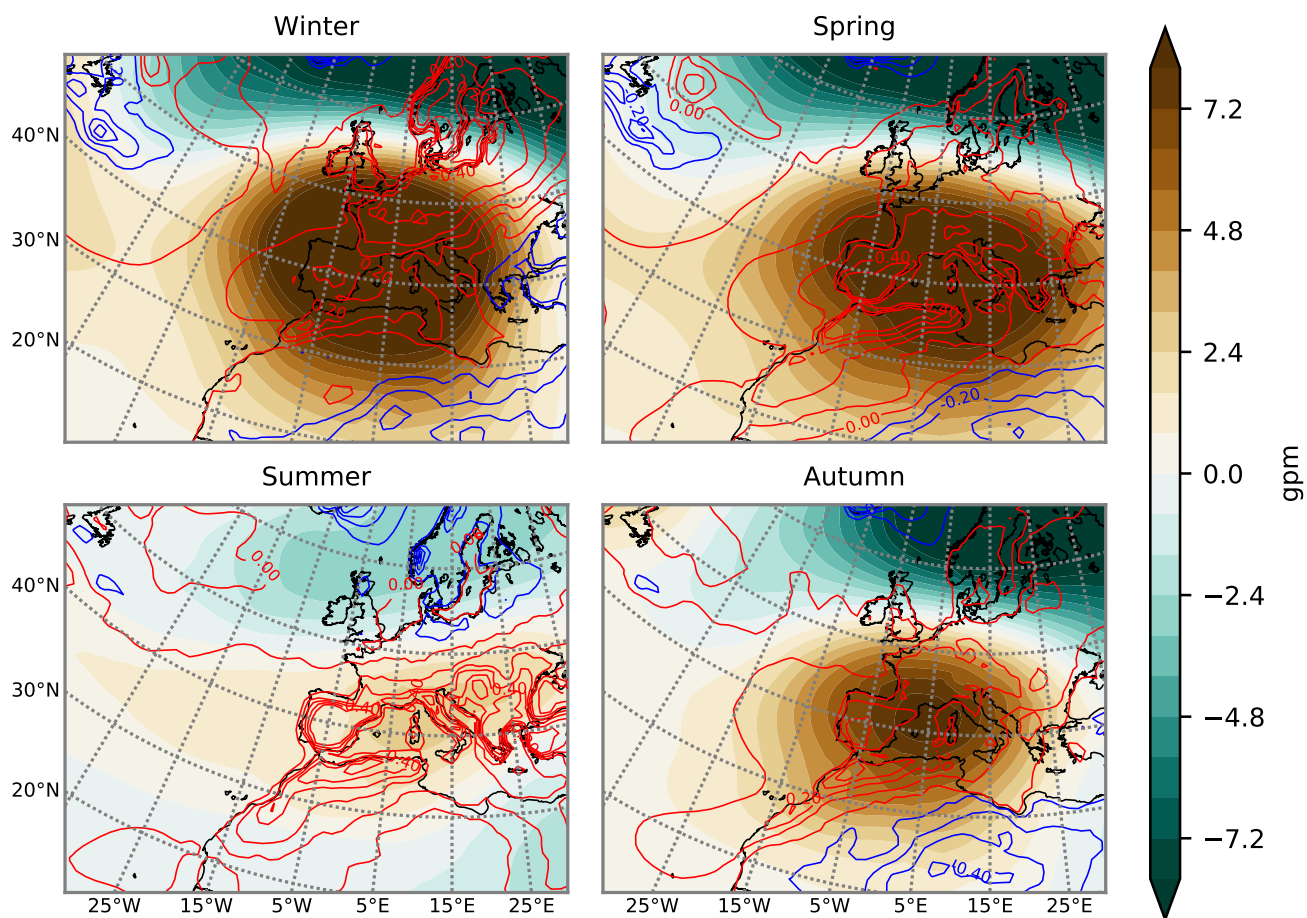


Figure 4. Mean geopotential height anomaly at 850 hpa (color shaded) and surface temperature anomaly (contours every 0.2°C , positive in red and negative in blue) during Mediterranean droughts for each season in the transient simulation.

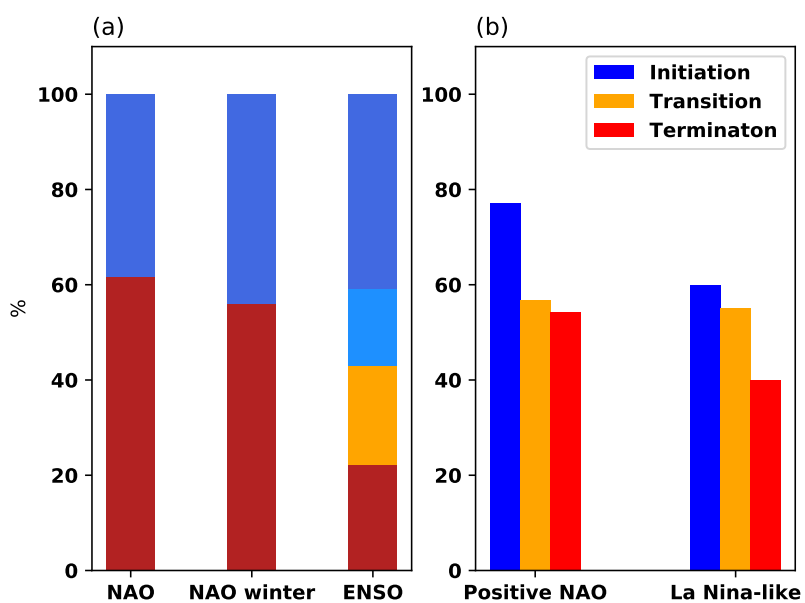


Figure 5. (a) Frequency of occurrence of positive (brown) and negative (blue) NAO, winter NAO and ENSO during Mediterranean droughts. In ENSO, the orange bar indicates neutral-positive (SST between 0 and 0.5 C°) and light blue is neutral-negative (SST between -0.5 and 0 C°) ENSO states. (b) Frequency of occurrence of positive NAO and La Nina-like condition during the initiation, transition and termination years of Mediterranean droughts.

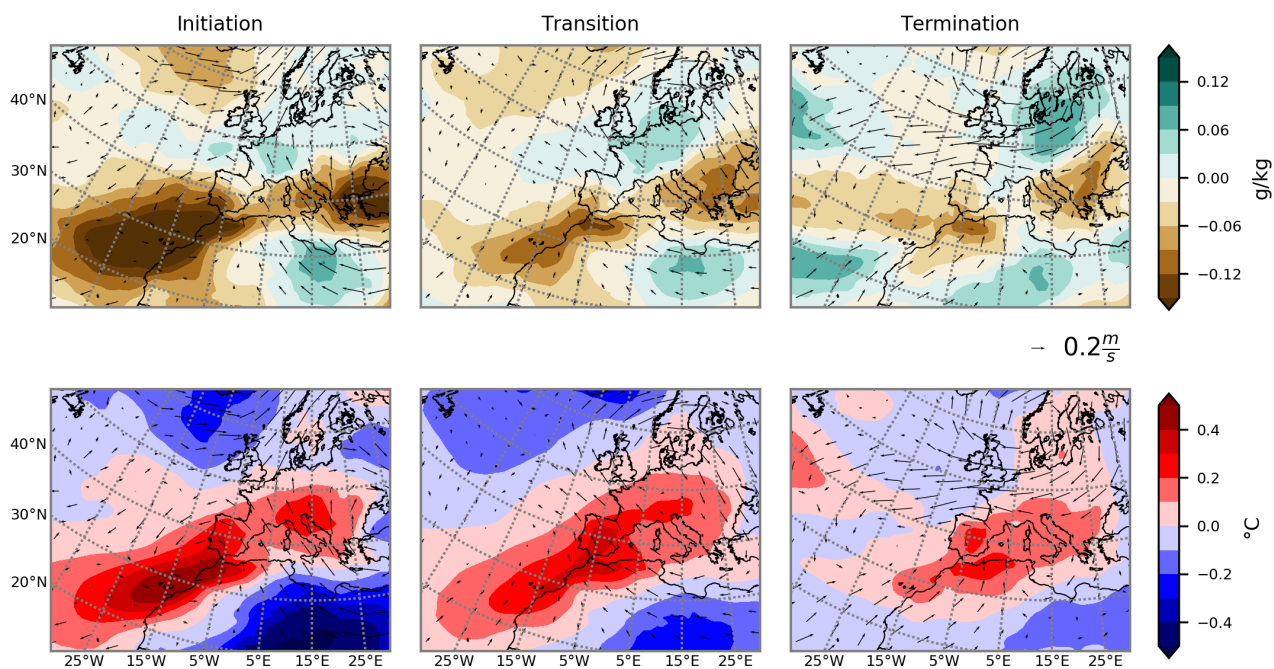


Figure 6. Evolution of atmospheric conditions during droughts with the positive NAO in the initiation year: anomalies of (above) specific humidity, and (below) temperature, both at 925 hPa during initiation, transition and termination years. Arrows indicate winds at 925 hPa.

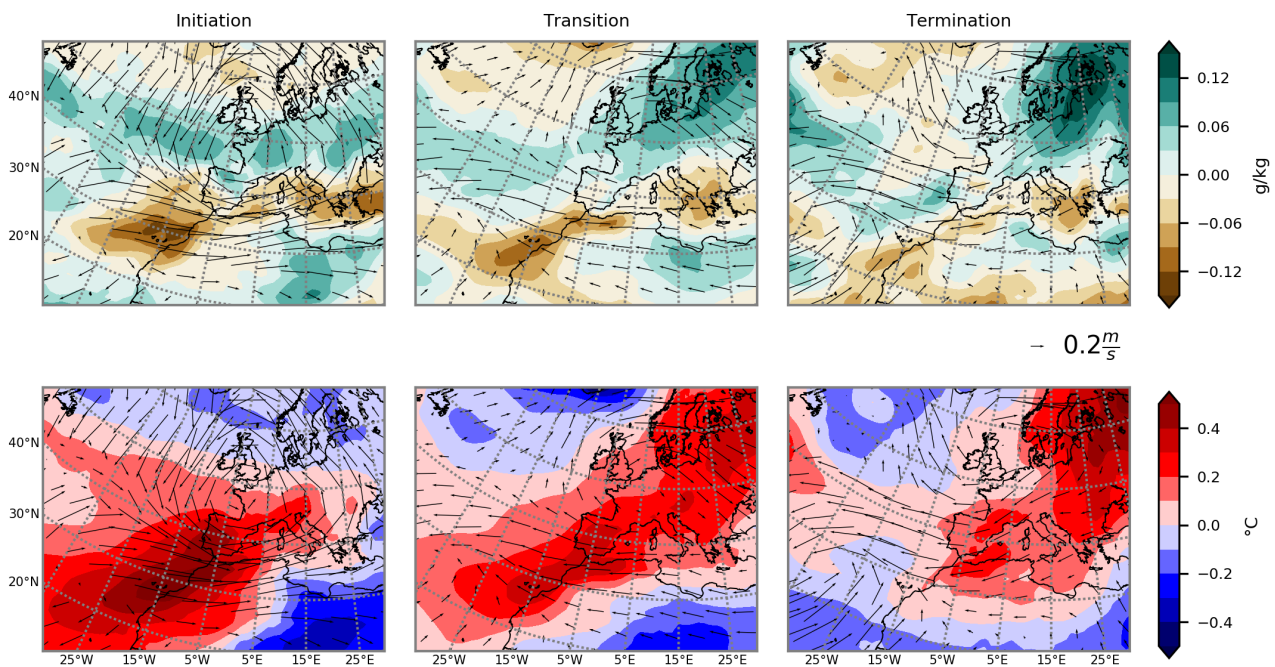


Figure 7. Same as Fig. 6 but with La Niña-like condition in the initiation year.

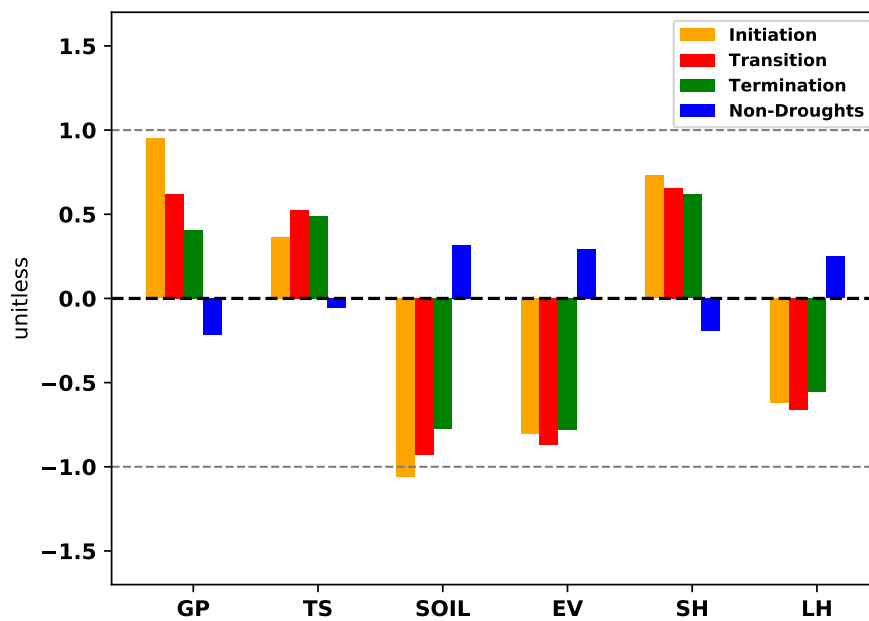


Figure 8. Standardized mean anomalies of geopotential height (GP), surface temperature (TS), soil moisture (SOIL), evapotranspiration (EV), surface sensible heat flux (SH), and surface latent heat flux (LH) during the initiation (yellow), transition (red) and termination (green) years of droughts over the region of study. The same variables during non-drought periods are shown in blue bars.

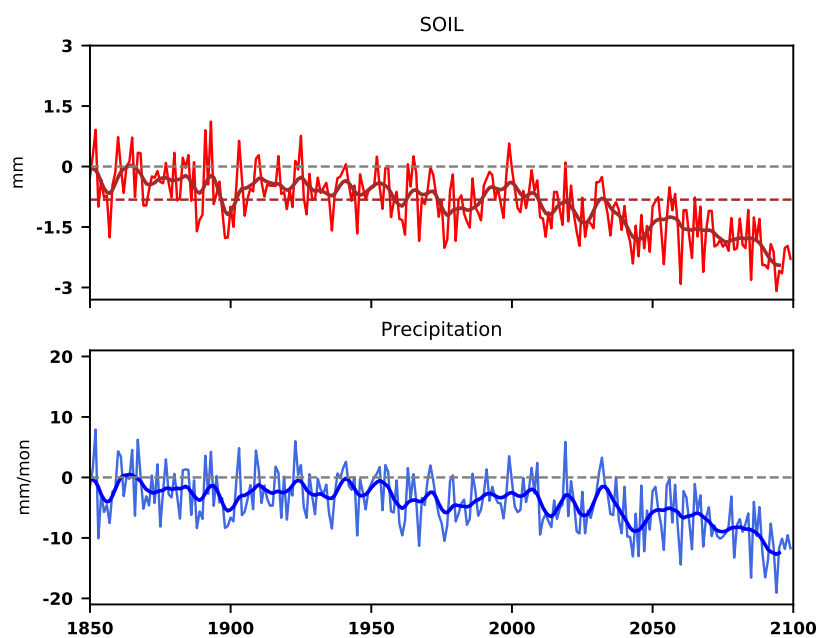


Figure 9. The time series of annual (above) soil moisture (SOIL), and (below) precipitation anomalies from 1850 to 2099 AD with respect to the 1000 - 1849 AD means.

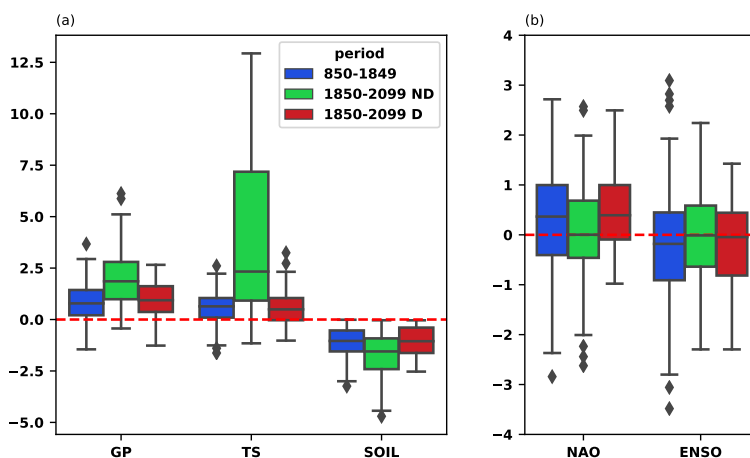


Figure 10. (a) Standardized regional variables: geopotential height at 850 hPa (GP), surface temperature (TS) and soil moisture (SOIL) anomalies over the region of study, and (b) indices of large scale circulation pattern: North Atlantic Oscillation (NAO) and SST over the NINO3.4 (ENSO) during Mediterranean droughts for the period of 850 - 1849 AD (blue), non-detrended 1850 - 2099 AD (green) and detrended 1850 - 2099 AD (red).

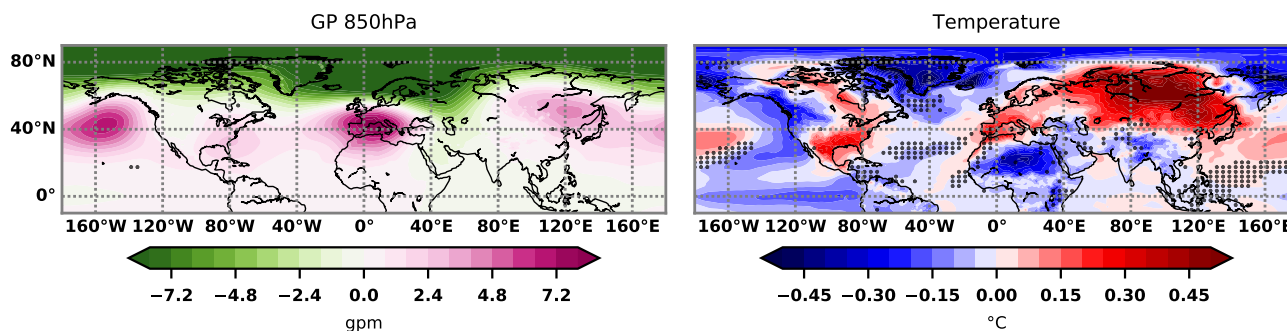


Figure 11. Detrended mean geopotential height anomaly at 850hpa and surface temperature anomaly during Mediterranean droughts for the 1850 - 2099 AD. Black dots indicate the regions where the means are statistically not significant at 5% confidence level with respect to the 850 - 1849 AD means (Fig. 3).